第 49 卷 第 11 期
2022 年 11 月

湖南大学学报（自然科学版）
Journal of Hunan University (Natural Sciences)
http://jonuns.com/index.php/journal/index

Vol. 49 No. 11
November 2022

Open Access Article https://doi.org/10.55463/issn.1674-2974.49.11.12

Improving the Corrosion Resistance of TNTZ in Hanks' Solution after Thermomechanical Treatment

Sir Anderson[1,2], Jon Affi[1], Yuli Yetri[2], Mitsuo Niinomi[3], Toshikazu Akahori[4], Gunawarman[1]*

[1] Department of Mechanical Engineering, Universitas Andalas, Padang, Indonesia

[2] Department of Mechanical Engineering, Politeknik Negeri Padang, Padang, Indonesia

[3] Institute for Materials Research, Tohoku University, Sendai, Japan

[4] Department of Material Science and Engineering, Graduate School of Science and Technology, Meijo University, Nagoya, Japan

Abstract: Ti-29Nb-13Ta-4.6Zr (TNTZ) is a new titanium alloy potentially to be used as bone implant material because of its advantages in terms of strength, ductility, non-toxicity, corrosion resistance, and biocompatibility. Its mechanical properties are suitable for bone applications; however, there are still problems related to its corrosion behavior when used for a long time. Therefore, this research aims to determine the corrosion rate and types, and provide corrosion prevention by applying the thermomechanical treatment on TNTZ in Hanks' solution. The limitation of this research was in not conducting the TNTZ biocompatibility tests. This research was conducted using the potentiodynamic polarization method in Hanks' solution as the corrosive medium at a temperature of 37°C and a pH of 6.8. Before corrosion testing, a TNTZ sample was treated with thermomechanical treatment combined with solution treatment at a temperature of 850°C and a holding time of 45 minutes, followed by rapid cooling (water quenching), and plastic deformation with deformation variations of 10%, 15%, and 20%, and it was ended with aging heat treatment at a temperature of 300°C and holding time for 1 hour. The novelties of this research are the valid data of corrosion rate and type of TNTZ, which were unavailable before, and corrosion prevention through thermomechanical treatment of TNTZ in Hanks' solution. The thermomechanical treatment is proved to reduce the pitting corrosion in TNTZ. The results show that thermomechanical treatment and increased plastic deformation can reduce the value of the corrosion rate, as evidenced by the pre-thermomechanical and thermomechanical TNTZ corrosion rates with deformation variations of 10%, 15%, and 20%, respectively, which were 5.522 x 10^{-4} mmpy; 2.754 x 10^{-4} mmpy; 2.290 x 10^{-4} mmpy; and 2.064 x 10^{-4} mmpy, respectively. TNTZ, after thermomechanical treatment, had the lowest corrosion rate, i.e., 2.064 x 10^{-4} mmpy, while Ti-6Al-7Nb had the highest one, i.e., 3.05 x10^{-2} mmpy. The type of TNTZ corrosion is pitting corrosion, as shown by the loss of zirconium that reduced the volume, causing pits to occur. Meanwhile, after thermomechanical treatment, pitting corrosion happened on TNTZ because of the loss or release of zirconium. This research shows that after thermomechanical treatment, TNTZ is the best material compared to other materials for biomedical applications based on corrosion resistance.

Keywords: titanium, TNTZ, corrosion, thermomechanics, deformation.

提高热机械处理后汉克斯溶液中天梯的耐腐蚀性

摘要：Ti-29Nb-13Ta-4.6Zr (天梯)是一种新型钛合金，具有强度、延展性、无毒、耐腐蚀和生物相容性等优点，有望用作骨植入材料。其机械性能适用于骨骼应用；但是，长期使用时，其腐蚀行为仍然存在问题。因此，本研究旨在确定腐蚀速率和类型，并通过在汉克斯

Received: July 11, 2022 / Revised: September 14, 2022 / Accepted: October 10, 2022 / Published: November 30, 2022

About the authors: Sir Anderson, Department of Mechanical Engineering, Universitas Andalas, Padang, Indonesia; Department of Mechanical Engineering, Politeknik Negeri Padang, Padang, Indonesia; Jon Affi, Department of Mechanical Engineering, Universitas Andalas, Padang, Indonesia; Yuli Yetri, Department of Mechanical Engineering, Politeknik Negeri Padang, Padang, Indonesia; Mitsuo Niinomi, Institute for Materials Research, Tohoku University, Sendai, Japan; Toshikazu Akahori, Department of Material Science and Engineering, Graduate School of Science and Technology, Meijo University, Nagoya, Japan; Gunawarman, Department of Mechanical Engineering, Universitas Andalas, Padang, Indonesia

Corresponding author Gunawarman, gunawarman@eng.unand.ac.id

溶液中对天梯进行热机械处理来提供腐蚀预防。这项研究的局限性在于没有进行天梯生物相容性测试。本研究采用动电位极化法，以汉克斯溶液为腐蚀介质，温度为 37°C，酸碱度值为 6.8。腐蚀试验前，对天梯样品进行热机械处理结合固溶处理，温度为 850℃，保温时间为 45 分钟，然后快速冷却（水淬），塑性变形，变形变化为 10%，15%和 20%，并在 300℃的温度和保持时间 1 小时的时效热处理结束。本研究的创新点在于获得了以前无法获得的天梯腐蚀速率和类型的有效数据，以及通过天梯在汉克斯溶液中进行热机械处理来防止腐蚀。事实证明，热机械处理可以减少天梯中的点腐蚀。结果表明，热机械处理和增加塑性变形可以降低腐蚀速率的值，如变形变化为 10%、15%和 20%的预热机械和热机械天梯腐蚀速率所证明的那样，分别为 5.522 x 10-4 毫米；2.754 x 10-4 平方毫米；2.290 x 10-4 平方毫米；和 2.064 x 10-4 mmpy，分别。热机械处理后的天梯的腐蚀速率最低，为 2.064 x 10-4 mmpy，而钛-6 阿尔-7 铌的腐蚀速率最高，为 3.05 x10-2 mmpy。天梯腐蚀的类型是点蚀，表现为锆的损失使体积减小，导致出现点蚀。同时，形变热处理后，由于锆的损失或释放，天梯发生点腐蚀。这项研究表明，经过热机械处理后，天梯与其他基于耐腐蚀性的生物医学应用材料相比是最好的材料。
关键词：钛、天梯、腐蚀、热力学、变形。

---

1. Introduction

Biomaterials are materials implantable in the human body for replacing damaged or defective tissues or organs [1]. They interact with biological systems and function as medical devices [2]. Those often used for implants to date are stainless steel type SUS 316L (ASTM F138) [3]-[5] and titanium (ASTM F136) [6]-[7] for their superior metallic mechanical properties and ease of manufacture. However, it is still necessary to consider their biocompatibility. 316 L stainless steel is preferable because it is cheaper than titanium [4]. However, it has weaknesses since it can harm bone and body health. One of its components, nickel, can be ionized and released into body fluids and cause allergies [5] and adverse effects on body health. It can cause hypersensitivity reactions, trigger cancer, and, of course, is toxic [8]. The allergic effects caused by nickel are related to corrosion. Corrosion is the release of metal ions into body fluids due to the tendency of the constituents to return to their original forms [9]. It can affect the ability of an implant to work for support, reposition, or help in the growth of new bone tissue. From the material viewpoint, it can decrease mechanical abilities, such as strength and hardness of the material, causing implantation failure. In this situation, titanium is better than 316 L stainless steel.

Currently, titanium is more attractive because, apart from being more corrosion resistant, it has advantages in terms of high strength and low modulus of elasticity [10] and good biocompatibility [11]. The most biocompatible type of titanium for implants is type ß, which comprises one or more alloying elements [11]. This type has the best corrosion resistance and a lower modulus of elasticity (closer to bone) than those of type α and type $\alpha+\beta$ [11]-[12]. Type ß titanium alloys have been widely developed for biomedical applications [11]-[12]. including Ti-29Nb-13Ta-4,6Zr (TNTZ) [13]. TNTZ has a low modulus of elasticity (58 Gpa) [14], closer to the modulus of elasticity of bone (30 Gpa). It has been developed to reduce the risk of stress-shielding implants in the shinbone [11].

TNTZ's compatibility with bone implants has been confirmed. However, no information on its service life when installed in the human body is available. A titanium alloy service life is the time it must survive in the human body until it undergoes corrosion, which is influenced by the body's fluids, such as salt, sweat, and blood. Several researchers have observed the corrosion of TNTZ using various solutions, such as Hanks [15]-[16], Kubokkos [17], and saliva [18]. However, studies using artificial body fluids close in composition to the body fluids, in this case Hanks' solution [19], only compared the corrosion resistance of TNTZ with those of CP-Ti [15] and Ti-15M0 [16] and did not determine TNTZ's corrosion rate. Thermomechanical treatment, for this reason, can be carried out to increase the corrosion resistance of TNTZ through a combination of heat treatment [20], the improvement of mechanical properties through mechanical treatment [21]-[22], and corrosion resistance [14], [23]. Related research carried out a combination of solution heat treatment, aging treatment, and mechanical treatment with the cold rolling process in 5% HCl solution on TNTZ and Ti-

30Nb-10Ta-5Zr [14]. This research was only to improve corrosion resistance, instead of for corrosion prevention. Other studies related to titanium alloys Ti-6Al-4V and Ti-6Al-2Mo-2Cr have combined heat treatment and mechanical treatment with the forging process [21], and Ti-6Al-4V treated with a combination of heat treatment and mechanical treatment with compression testing [22], but only limited to increase in strength without analyzing the corrosion behavior.

To overcome the shortcomings of previous studies in looking at the effect of thermomechanical treatment, increasing the corrosion resistance of TNTZ in Hanks' solution can be done by combining solution heat treatment, aging treatment, and mechanical treatment with a compression test. This research aimed to obtain TNTZ with optimal corrosion-resistant properties implantable in the human body for a long time.

This research was to determine the corrosion behavior and the type of corrosion of TNTZ in Hanks' solution and increase, by knowing the corrosion prevention technique through thermomechanical treatment, the corrosion resistance of TNTZ to be potential as an alternative material for biomedical applications (bone implants).

2. Materials and Method

2.1. Sample Preparation, Thermomechanical Treatment, and Test Solution

The pre-thermomechanical and thermomechanical post-corrosion samples were prepared with 10%, 15%, and 20% deformations, each of 4 pieces. Cylindrical samples were cut with an average thickness of 3 mm and an average diameter of 6 mm. The surfaces were then leveled using sandpaper starting from 400, 800, 1200, 1500, 2000, and up to 5000 mesh.

The samples were treated with thermomechanical treatment, namely by a combination of solution heat treatment (ST), mechanical loading with a compression test, and aging treatment (AT). The heating process was carried out using the Nabertherm GmbH (Germany) furnace at a maximum temperature of 1280ºC. The solution treatment was carried out by heating to a temperature of 850ºC, a temperature increase interment of 10ºC/s, and holding time of 60 minutes [24], followed with rapid cooling using water or water quenching (WQ). The next step was the compression test carried out by pressing the samples in the axial direction at room temperature (27ºC) using the Jinan Precision Universal Testing Machine with a maximum capacity of 300 kN and deformation variations of 10%, 15%, and 20%. Then, it was followed with the aging process, by reheating at a temperature of 300ºC and a holding time of 1 hour, followed with slow cooling at room temperature [25]. The schematic of the thermomechanical process can be seen in Figure 1.

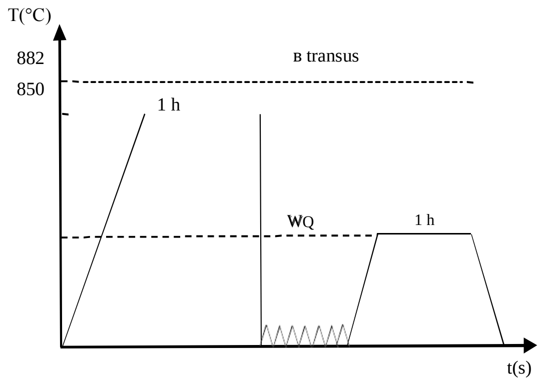

Figure 1. Schematic of the thermomechanical process

Calculation of plastic deformation using Equation (1) [26]:

$$\varepsilon = \frac{\Delta h}{ho} x\ 100\% \quad (1)$$

$$\Delta h = h_o - h_i$$

Note: h_i is the final height (mm), h_o is the initial height (mm), Δh is the change in height (mm), ε is a plastic deformation (%). The change in height due to plastic deformation is measured using a dial indicator equipped with a magnetic stand.

Before the corrosion treatment, the samples' surfaces were soldered against the tip of a conducting wire to allow current to flow during the test. The next step was mounting the samples using resin so that the solution only contacted the lower surfaces, which were polished using 8000 and 14000 mesh to make them smooth, shiny, and free from scratches.

The body simulation solution used was Hanks' solution with a pH of 6.8 as a corrosive solution because it was closest to the composition of the human body, as shown in Table 1.

Table 1 Hanks' solution composition

Element	NaCl	KCl	$CaCl_2$	$NaHCO_3$	$MgCl_2.6H_2O$	$MgSO_4.7H_2O$	Na_2HPO_4	KH_2PO_4	Glucose. $2H_2O$
g/l	8	0.40	0.14	0.35	0.60	0.06	0.06	0.60	1.0

2.2. Sample Examination of Surface Morphology and Chemical Composition

The morphological examination of the surfaces of the test objects was performed out using SEM (Scanning Electron Microscope) Hitachi S-3400N EMAX X-Act series to determine corrosion marks and the type of corrosion, while the chemical composition was measured using Energy Dispersive X-ray (EDX).

2.3. Corrosion Testing with a Potentiostat Polarization Method

To determine the active-passive behavior of the sample, a corrosion test was performed using a potentiodynamic technique (potentiostat) in Hanks' solution at 37°C. The electrodes used were working electrodes, reference electrodes, and auxiliary electrodes, namely: Pt. Ag/AgCl, and steel. The three electrodes were immersed in Hanks' solution, then connected to a potentiostat and adjusted the potential to obtain a curve of the relationship between potential (E) vs current (I).

The Origin software test results show the Tafel curve to determine the Icorr value and the Ecorr value by making a straight-line equation on the Tafel curve so that the lines intersect. When a vertical line was drawn, the Icorr value was obtained at the intersection point, and when a horizontal line was drawn at the intersection point, the E value was also shown by the Origin software. The I_{corr} value was entered into the corrosion rate calculation using Equation (ASTM vol 03.02.G02) (2).

$$CR = K_1 \frac{I_{coor}}{\rho} EW \quad (2)$$

where CR is the corrosion rate (mmpy), I_{corr} is the current density, K_1 is a constant with a value of 3.27 x 10^{-3} mm. g/µA.cm. yr, EW EW is the equivalent mass with a value of 11.98, is the density (g/cm^3).

2.4. Flowchart of Research Stages

Figure 2 shows a flowchart of this study.

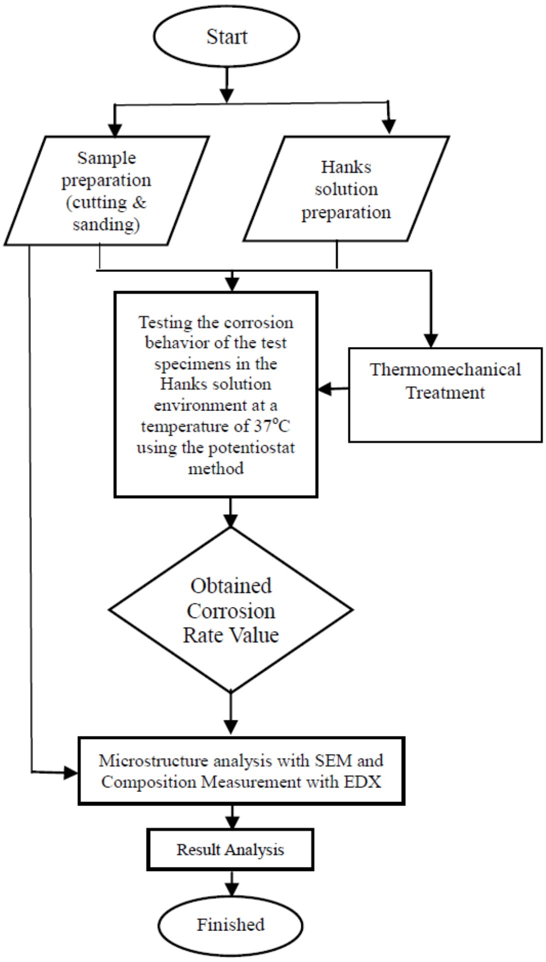

Fig. 2 Research flowchart

Experiment was started with the preparation of TNTZ sample materials by cutting into sizes according to predetermined dimensions and sanding before preparing Hanks' solution. After the solution was ready, the sample's microstructure and chemical composition were examined to get initial data before corrosion testing. The next step was the application of thermomechanical treatment, followed by the corrosion test of the test specimens, which performed out in the Hanks' solution environment at a temperature of 37°C using the potentiostat method before and after thermomechanical treatment. After determining the corrosion rate, TNTZ's microstructure and chemical composition of were examined to determine the type of corrosion that occurred. The data were then analyzed to determine the effect of the thermomechanical process on the corrosion rate and the type of corrosion.

3. Results and Discussion

3.1. Pre-Corrosion Treatment Characteristics

Regarding the characteristics of TNTZ before corrosion, an SEM test was performed out to determine the initial composition of the material used.

The results of the surface morphology examination using SEM can be seen in Figure 3. The SEM results show that there is no corrosion in TNTZ.

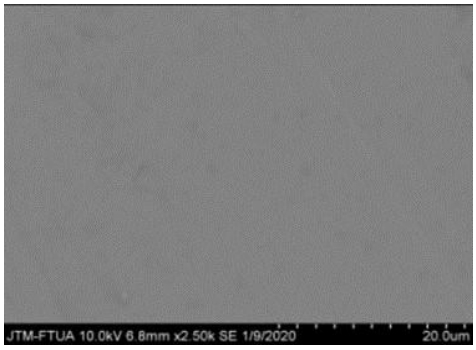

Fig. 3 TNTZ SEM results

The test results for the chemical composition of TNTZ can be seen in Table 2. The main element of TNTZ is titanium, as evidenced by the largest percentage by weight mass is titanium Ti, reaching 53.04% of the total mass. In addition to titanium, other elements are resistant to corrosion without the presence of nickel. TNTZ contains niobium, tantalum, and zirconium by 30.94%, 12.42%, and 3.60%, respectively, by mass. The measurement results prove that the material is TNTZ because it is almost the same in the literature as titanium, niobium, tantalum, and zirconium elements by 53.009%, 29%, 13.3%, and 4.66%, respectively, by mass [26].

Table 2 Chemical composition of TNTZ

TNTZ		
Element	**Mass %**	**Atom %**
Ti	53.04	72.43
Nb	30.94	21.78
Ta	12.42	5.79
Zr	3.60	1.90
Total	100%	

3.2. Pre-Thermomechanical Corrosion Characteristics

3.2.1. Corrosion Rate

The corrosion rate value was obtained using the potentiodynamic polarization method (potentiostat) which was carried out based on Tafel analysis with a current of 1 mV every 1 second. The data obtained were processed in the Origin software, so that the Tafel curve was obtained on the y-axis for the current plotted on a logarithmic scale and the x-axis for the voltage used during the corrosion process, as shown in Figure 4, using 4 TNTZ samples.

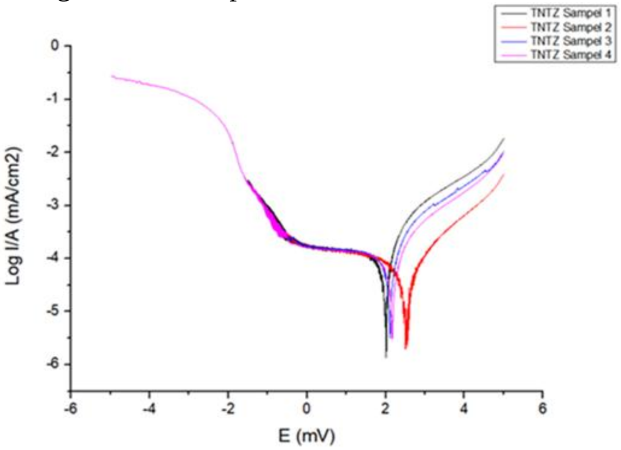

Fig. 4 TNTZ Tafel curve

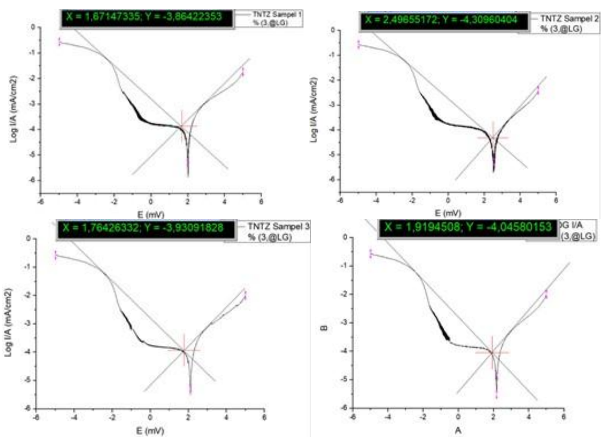

Fig. 5 I_{corr} and E_{corr} of the TNTZ Tafel curves of (a) sample 1, (b) sample 2, (c) sample 3, and (d) sample 4

The Tafel curve shows the anodic region on the left and the cathodic region on the right. In the anodic region, during the corrosion process, the current given gets bigger while the voltage gets smaller until it reaches the saturation point. In the cathodic region, the opposite occurs; the current applied is directly proportional to the voltage. Furthermore, using the Origin software, from the Tafel curve, the values of the corrosion current density (I_{corr}) and the corrosion voltage (E_{corr}) were determined by making a straight-line equation on the Tafel curve tangent to the curve so that the lines intersect. At the point of intersection of the tangents, I_{corr} was obtained when a horizontal line was drawn, and E_{corr} was shown when a vertical line was drawn at the intersection point, as shown in Figure 5.

I_{corr} of the Tafel polarization curve was incorporated into the calculation of the corrosion rate using Equation 2 (ASTM vol 03.03.G02). The results of the calculations using equation 2 can be seen in Table 3.

Table 3 shows that the I_{corr} value obtained from the Tafel curve was directly proportional to the corrosion rate; the smaller the Icorr, the lower the corrosion rate. This finding is in line with the results of previous studies [15], [16].

Table 3 I_{corr}, E_{corr}, and TNTZ corrosion rate

Test	I_{corr} (A/cm^2)	E_{corr} (mV)	CR (mmpy)
1	1.367 x 10^{-7}	1.67	7.539 x10^{-4}
2	5.011 x 10^{-8}	2.47	3.321 x 10^{-4}
3	1.132 x 10^{-7}	1.77	6.159 x 10^{-4}
4	9.179 x 10^{-8}	1.90	5.071 x 10^{-4}
Average	9.797 x 10^{-8}	1.95	5.522 x 10^{-4}

Several materials' corrosion rates were studied previously using Hanks' solution with the same method as shown in Figure 6 to see more clearly the comparison of the corrosion rates.

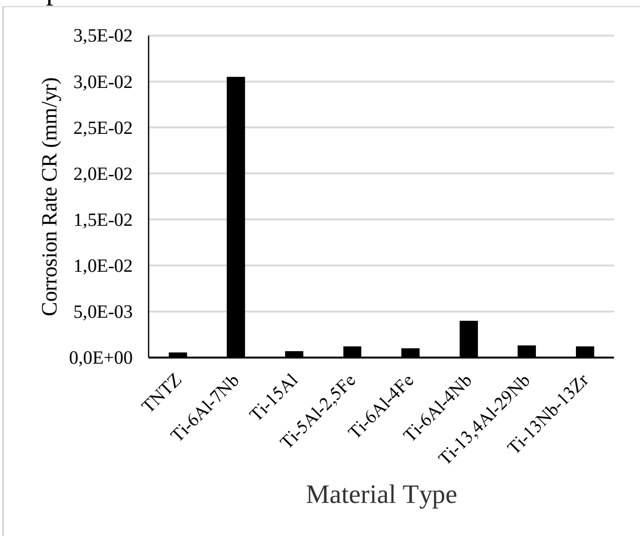

Fig. 6 Comparison of corrosion rates in Hanks' solution

The materials studied were Ti-6Al -7Nb [27], Ti-15Al, Ti-5Al-2,5Fe, Ti-6Al-4Fe, Ti-6Al-4Nb, Ti-13,4Al-29Nb, Ti-13Nb-13Zr [28]. The material with the lowest corrosion rate, which was 5.522 x 10-4 mm/yr, was TNTZ, while the one with the largest value, 3.05 x 10-2 mm/yr, was Ti-6Al-7Nb. This phenomenon occurred since the material with a lower corrosion rate released fewer atoms during corrosion [29]. Additionally, the alloying elements contained in TNTZ, such as Nb, Ta, and Zr, apart from being isomorphous stabilizing elements, function and are used to increase corrosion resistance [30].

Meanwhile, studies on the corrosion of TNTZ using artificial body fluids, in this case, Hanks' solution [19], which is similar to natural body fluids in terms of composition, have only been limited to comparing the corrosion resistance of TNTZ with those of CP-Ti [15] and Ti-15M0 [16] and have not determined the value of their corrosion rates.

3.2.2. Corrosion Type

The type of corrosion in TNTZ was determined by examining the surface morphology and composition. The results of surface morphology examination using an optical microscope on the upper surface of TNTZ after corrosion treatment in Hanks' solution can be seen in Figure 7.

(a)

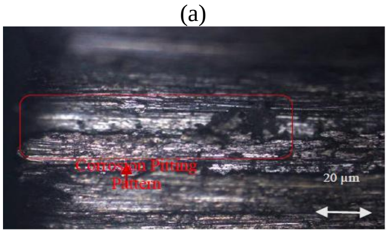

(b)

Fig. 7 Optical microscope photo of TNTZ: (a) Top surface; (b) Transverse surface pitting corrosion pattern

Figure 7 (a) shows that corrosion occurred on the surface of the TNTZ sample is in the form of black perforated spots. Meanwhile, Figure 7 (b) shows that corrosion spreads into the material on the transverse surface. The shape of the spread was like a line spreading inward and widening inside. Based on the form of the spreading, the corrosion was categorized as pitting corrosion, which can reduce the volume of the material, as shown by the volume missing.

After examining the surface morphology, a chemical composition examination with EDX was carried out on the top and transverse surfaces of TNTZ to ensure the corrosion in the observation area and the type of corrosion. The results of the TNTZ composition test are presented in Table 4 on the upper surface and Table 5 on the transverse surface. Table 4 shows the appearance of oxygen in each spectrum on the material surface after corrosion testing. The first, second, and third spectra showed 32.68%, 18.26%, and 24.92%, respectively. The first spectrum contained oxygen as the largest one compared to the others, indicating that in that area, the material surface-experienced corrosion dominated by oxygen. In each spectrum, apart from oxygen, TNTZ elements, such as titanium (Ti), niobium (Nb), and tantalum (Ta), were significantly reduced after corrosion, while zirconium (Zr) was not reduced by oxygen. Other elements in Hanks' solution, such as magnesium (Mg), appeared on the material surface due to the attachment or adsorption between the TNTZ's surface and the solution during the corrosion process, letting the elements of the solution to bind during the reaction.

Table 4 Results of examination of the chemical composition of the post-corrosion TNTZ surface

TNTZ						
Element	**Spectrum 1**		**Spectrum 2**		**Spectrum 3**	
	Mass %	**Atom %**	**Mass %**	**Atom %**	**Mass %**	**Atom %**
O	32.68	62.32	18.26	45.86	24.92	54.85
Mg	1.98	2.48	-	-	-	-
Si	6.49	7.05	4.20	6.01	5.43	6.81
Ti	31.75	20.23	41.58	34.88	37.99	27.93
Nb	20.95	6.88	25.03	10.82	23.05	8.74
Ta	6.15	1.04	10.92	2.42	8.61	1.68
Total	100%		100%		100%	

In Table 5, the transverse surface also shows the appearance of oxygen in the first spectrum of 9.22% and the loss of zirconium (Zr), which was initially 3.60%, in all spectra. This phenomenon indicates that corrosion had occurred. The loss of zirconium (Zr) triggered the release of metal ions and caused weight/volume loss so that pits appeared in TNTZ, resulting in pitting corrosion.

Table 5 Results of examination of the chemical composition of the post-corrosion TNTZ transverse surface, pitting corrosion

TNTZ						
Element	**Spectrum 1**		**Spectrum 2**		**Spectrum 3**	
	Mass %	**Atom %**	**Massa %**	**Atom %**	**Mass %**	**Atom %**
O	9.22	26.48	-	-	-	-
Mg	-	-	-	-	-	-
Si	1.28	2.10	1.94	3.86	1.52	3.04
Ti	61.10	58.61	68.45	79.88	69.36	81.32
Nb	23.25	11.50	24.28	14.61	22.46	13.58
Ta	5.14	1.31	5.33	1.65	6.66	2.07
Total	100%		100%		100%	

Another study that examined TNTZ material in Kubokkos solution found that the surface of TNTZ was the same, i.e., blackish spots with pits indicating pitting corrosion, but the shape of the spreading like an ellipse was not too deep to spread inward [17]. Meanwhile, in Hanks' solution, the spreading form is like a line spreading inward and widening inside. Here, Hanks' solution was more corrosive than the Kubokkos solution because the amount of chloride compounds that caused corrosion was higher in Hanks' solution, in which NaCl = 8 g/l, KCl = 0.40 g/l, $MgCl_2.6H_2O$ = 0.60 g/l [Table 1], while in the Kubokkos solution, NaCl = 7.9 g/l, KCl = 0.22 g/l, $MgCl_2.6H_2O$ = 0.30 g/l [17]. The results of the composition examination using EDX in Table 3 show the appearance of the average oxygen of each spectrum of 25% and the reduction of titanium, niobium, and tantalum to 36%, 23%, and 5.7%, respectively, in Hanks' solution.

Meanwhile, in the Kubokkos solution, as shown in Table 6, oxygen appeared to be less than 5%, and titanium, niobium, and tantalum were slightly reduced to 44.77%, 26.16%, and 13.11%, respectively. These reductions of titanium, niobium, and tantalum in Hanks' solution triggered the release of metal ions, causing weight/volume loss and making the pits deeper.

However, in the 3% NaCl solution, uniform corrosion appeared because the corrosion test was not performed out using the potentiostat method but only an immersion test for up to 6 weeks at room temperature, instead of body temperature. Therefore, pitting did not appear.

Table 6 Chemical composition of TNTZ after corrosion [17]

Balance	%Nb	%Ta	%Zr	Impurities				
				%C	**%O**	**%Na**	**%Si**	**%Cl**
44.77	26.16	13.11	0	0-51.34	1.59-58.74	0-8.59	0-45.89	0-7.61
				%K	**%Sn**	**%Fe**	**%Cu**	**%Zn**
				0-6.1	0-3.45	0-0.66	0-44.01	0-23.68
				%W	**%N**	**%Al**	**%S**	**%Ca**
				0-2.42	0-17.27	0-0.36	0-0.8	0-1.44

3.3. Post-Thermomechanical Corrosion Characteristics

In this study, TNTZ was subject to pitting corrosion. To increase its corrosion resistance and eliminate pitting corrosion (corrosion prevention), a thermomechanical process, therefore, was performed out in 3 stages: solution heat treatment (ST), mechanical loading a compression test, and aging treatment (AT).

The uneven distribution of elements in titanium alloys is one of the causes of pitting corrosion. TNTZ is an alloy with elements and high contents, bringing it to experience multiple element separation and uneven element distribution that cause pitting corrosion. Thermomechanical treatment, in this case, can increase the occurrence of homogenization and reduce separation [14], thereby increasing the corrosion resistance. The treatment includes solution heat treatment (ST), mechanical loading by compression test, and aging treatment (AT). In the solution treatment process, the alloy is heated at a temperature of 850°C and held for 60 minutes until it forms a complete solid solution (that is, the single-phase region on the phase diagram). The matrix phase state at this temperature allows the elements to diffuse into the parent matrix and distribute themselves evenly [31]. The composition occurring is referred to as a solid solution, which is then rapidly quenched until it reaches room temperature and remains evenly distributed [31].

On mechanical loading with a compression test, deformation occurs and causes a strain hardening mechanism, which causes the dislocations to deform and accumulate at the grain boundaries [32]. This accumulation makes the dislocations heavier to move, requiring higher shear stress to move the dislocations. This mechanism causes the material to strengthen so that the gap between the grains becomes smaller, resulting in a slowdown of the corrosion process and increasing the material's corrosion resistance. The greater the deformation, the more dislocations deformed and accumulated at the grain boundaries, and the higher the corrosion resistance. Additionally, plastic deformation causes the alloy grains to break, triggering the phenomenon of recrystallization (grain growth) [32]. The increase in plastic deformation given to the alloy causes the alloy structure to become tighter. Due to the quenching, alloys with supersaturated solid solution structures tend to be unstable and form Mg_2Si precipitates [31]. Therefore, aging treatment process functions to let Mg_2Si dispersed and precipitated by reheating the solution at a temperature of 300°C and holding it at that temperature for 1 hour. The alloy is heated to accelerate the formation of the precipitates and make them stable, thereby strengthening the alloy itself.

3.3.1. Post-Thermomechanical Corrosion Rate

After the thermomechanical process, the corrosion rate was tested using the potentiostat polarization method. The results of the corrosion rate test using the potentiostat polarization method obtained Tafel curves for each of the 4 samples at 10%, 15%, and 20% deformations for TNTZ, as shown in Figure 8.

The TNTZ Tafel curve in Figure 7 shows that the trends of the curves before the thermomechanical and deformation processes of 10%, 15%, and 20% are downwards. This phenomenon reveals that the corrosion resistance is better after a thermomechanical process, as previous studies did [14]. The lower the Tafel curve, the higher the corrosion resistance [15, 16]. In addition, the greater the deformation carried out in the thermomechanical process, the better the corrosion resistance.

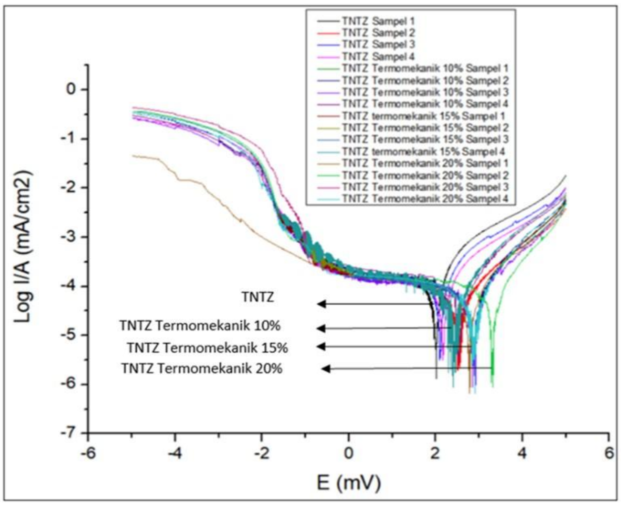

Fig. 8 TNTZ thermomechanical treatment Tafel curve

From the Tafel curve, the I_{corr} value, which was used to calculate the corrosion rate using Equation (ASTM vol 03.03.G02), was obtained. The results of the calculations with Equation 2 can be seen in Table 7.

Table 7 TNTZ thermomechanical corrosion rates

Deformation	Test	I_{corr} (A/cm^2)	E_{corr} (mV)	CR (mmpy)
0%	1	4.915 x 10^{-8}	2.76	2.271 x 10^{-4}
	2	5.075 x 10^{-8}	2.77	2.697 x 10^{-4}
	3	4.739 x 10^{-8}	2.77	2.441 x 10^{-4}
	4	6.610 x 10^{-8}	2.47	3.609 x 10^{-4}
	Average	5.335 x 10^{-8}	2.69	2.754 x 10^{-4}
15%	1	4.451 x 10^{-8}	2.80	1.963x 10^{-4}
	2	4.177 x 10^{-8}	2.81	1.937x 10^{-4}
	3	4.591 x 10^{-8}	2.80	2.367 x 10^{-4}
	4	5.517 x 10^{-8}	2.40	2.895 x 10^{-4}
	Average	4.684 x 10^{-8}	2.70	2.290 x 10^{-4}
20%	1	5.381x10^{-8}	2.81	2.135 x 10^{-4}
	2	4.605 x 10^{-8}	3.36	2.324 x 10^{-4}
	3	4.473 x 10^{-8}	2.86	1.970 x 10^{-4}
	4	4.004 x 10^{-8}	2.83	1.826 x 10^{-4}
	Average	4.616 x 10^{-8}	2.96	2.064 x 10^{-4}

The results of Tables 3 and 7 were made in bar charts, and the standard deviation values were calculated, as shown in Figure 9.

The results of Table 3, Table 7, and Figure 9 reveal the average corrosion rates before and after thermomechanics with deformations of 10%, 15%, and 20%, respectively, in Hanks' solution of 5.522 x 10^{-4} mmpy, 2.754 x 10^{-4} mmpy, 2.290 x 10^{-4} mmpy, and 2.064 x 10^{-4} mmpy.

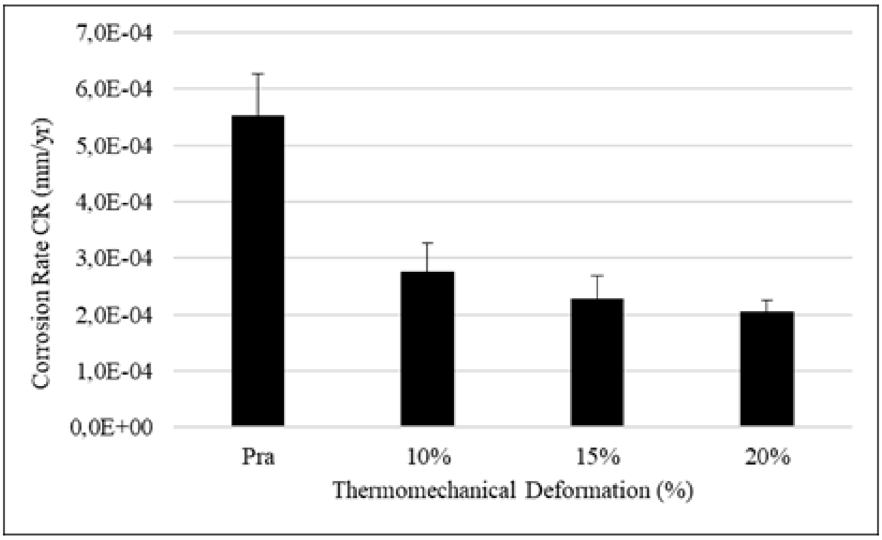

Fig. 9 TNTZ thermomechanical treatment corrosion rates

Data on the corrosion rates show a significant decrease in the value of the corrosion rate before and after thermomechanics. This condition shows that the corrosion resistance increased quite high. As for the thermomechanical treatment, the greater the deformation, the lower the corrosion rate, but the decrease was not too high. This means that corrosion resistance increases when deformation increases because the TNTZ constituent elements, namely, titanium, niobium, tantalum, and zirconium, can facilitate the formation of small gaps or pores. Therefore, before the thermomechanical process on TNTZ, the pores into which the ions contained in Hanks' solution enter still exist, thereby causing corrosion. The thermomechanical treatment can reduce the pores, preventing the ions in Hanks' solution from entering, thereby reducing the corrosion process.

3.3.2. Type of-Post Thermomechanical Corrosion

The post-thermomechanical TNTZ surface morphology examination using SEM in Figure 10 shows black spots, indicating the occurrence of corrosion. The form of corrosion, which was not obviously visible as pits on the surface, indicates pitting corrosion in post-thermomechanical TNTZ.

Figures 10 (a), (b), and (c) illustrate that the greater the deformation of the thermomechanical treatment, the fewer the blackish spots, meaning that the corrosion decreased. These findings were also in line with the results of corrosion rate testing with a potentiostat on post-thermomechanical TNTZ, as shown in Table 7 and Figure 10, indicating that the higher the deformation, the lower the corrosion rate.

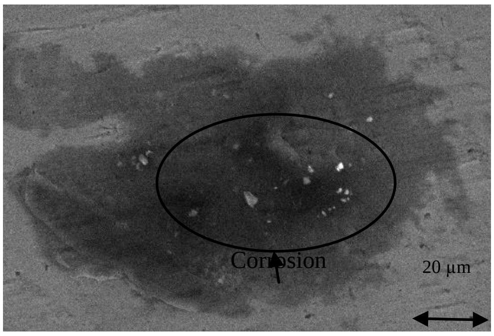

(a)

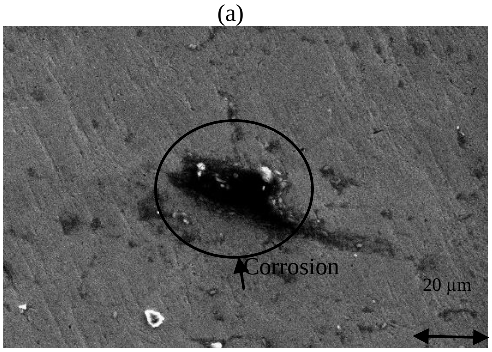

(b)

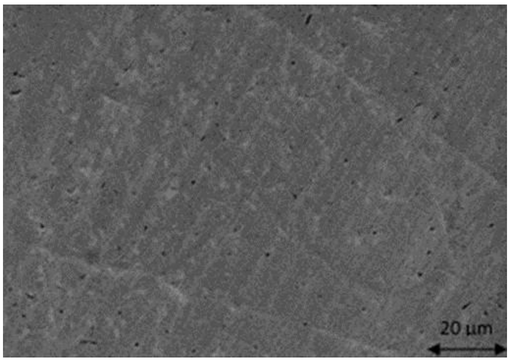

(c)

Fig. 10 SEM photo of TNTZ post thermomechanical deformations of (a) 10% (b) 15% (c) 20%

After examining the surface morphology, an examination of the composition of the TNTZ after thermomechanical treatment was carried out. Table 8 describes the results of the thermomechanical treatment with 10% deformation. The reduced atomic masses of the elements of titanium, niobium, tantalum, and zirconium were replaced by the appearance of oxygen of 17.83%, 13.71%, and 17.72% in spectra 1, spectra 2, and spectra 3, respectively, indicating that corrosion had occurred. Table 8 also shows that the greater the deformation because of the thermomechanical treatment, the smaller the oxygen appears 10.85%, 16.64%, and 15.52% at the 15% deformation in spectrum 1, spectrum 2, and spectrum 3, respectively, and 17.53%, 13.15%, and 13.36% at the 20% deformation in spectrum 1, spectrum 2, and spectrum 3, respectively. These data show that the greater the deformation, the lower the corrosion rate, as indicated by the corrosion rate test with a potentiostat, as shown in Table 7 and Figure 9.

Table 8 shows the presence of Si element impurities, while the elements in Hanks' solution had not yet appeared in the thermomechanical TNTZ. In post-corrosion pre-thermomechanics, Hanks' solution element, namely, Mg in TNTZ, appeared, as shown in Table 4. This phenomenon indicates that thermomechanical treatment increases TNTZ's corrosion resistance. The results of this study were also in line with previous studies regarding the thermomechanical treatment of TNTZ in a corrosive 5% HCL solution [14]. However, these studies compare corrosion resistance without determining the corrosion rates. The solution treatment process on TNTZ was carried out by heating to a temperature of 1063 K for 3.6 ks, followed by water quenching (WQ). Aging treatment was performed by heating at a temperature of 673 K for 259.2 ks. Furthermore, mechanical loading was carried out using cold rolling treatment with plastic deformation up to 87.5%. The corrosion resistance of TNTZ with thermomechanical treatment was better than those of Ti-30Nb-10Ta-5Zr & TNTZ ST without thermomechanical treatment in 5% HCL corrosive solution [14].

The results of the surface morphology examination only showed blackish spots that did not look too perforated. However, the examination of the post-thermomechanical chemical composition of TNTZ, as shown in Table 8, showed no visible appearance of zirconium reduced by oxygen in the entire spectra. Therefore, in post-thermomechanical TNTZ, pitting corrosion still occurred although the corrosion resistance increased. However, thermomechanical treatment could reduce pitting corrosion, as evidenced by the relatively small number of pits. The results of the EDX examination in Table 8 show that the elements released post-corrosion were less than those before thermomechanical treatment.

3.3.3. Material Density and Thermomechanical Treatment Mechanism

Based on the research's results, the mechanism of the corrosion process in TNTZ can be assumed to occur through a series of stages. In the first stage, the material received from the factory (as received) had macro defects in fine pits (pores) that looked like gaps. This was probably due to the relatively large number of elements that made up the TNTZ alloy material, namely, titanium, niobium, tantalum, and zirconium, that supported the formation of small gaps or pores. At the next step, the liquid entered the material through the fine pores, causing a corrosion process when the TNTZ alloy material was immersed in Hanks' solution. The corrosion process in TNTZ indicated a spontaneous electrochemical reaction, which caused the release of metal ions and caused damage to metal implants. The electrochemical process is a combination of metal oxidation reactions, which, in this case, involved TNTZ at the anode and the reduction reaction of oxygen molecules in Hanks' solution at the cathode.

Table 8 The results of the examination of TNTZ chemical composition after thermomechanics

Thermomechanical deformation		**Spectrum 1**		**Spectrum 2**		**Spectrum 3**	
	Element	**% Mass**	**% Atoms**	**% Mass**	**% Atoms**	**% Mass**	**% Atoms**
10 %	O	17,83	42,54	13,71	39,23	17,72	47,00
	Si	4,49	6,10	-	-	-	-
	Ti	50,31	40,10	46,48	44,42	42,76	37,87
	Nb	27,38	11,25	26,19	12,91	26,36	12,04
	Ta	-	-	13,61	3,44	13,16	3,09
	Total	100%		100%		100%	
15 %	O	10,85	33,36	16,64	40,89	15,52	37,82
	Si	-	-	4,54	6,36	4,75	6,77
	Ti	46,14	47,36	35,33	36,64	38,39	39,74

Continuation of Table 8

	Nb	29,51	15,62	30,03	12,71	28,52	12,29
	Ta	13,51	3,67	13,46	3,41	13,24	3,39
	Total	100%		100%		100%	
20 %	O	17,53	42,03	13,15	38,32	13,36	38,49
	Si	4,76	6,50	-	-	-	-
	Ti	36,45	36,53	45,41	44,21	46,61	44,84
	Nb	27,73	11,45	27,81	13,96	26,82	13,30
	Ta	13,52	3,48	13,63	3,51	13,21	3,36
	Total	100%		100%		100%	

The following are oxidation and reduction reactions between TNTZ metals in Hanks' solution:

Oxidation: $M \rightarrow M^{2+} + 2e^-$

Reduction: $\frac{1}{2} O_2 + 2e^- + H_2O \rightarrow 2OH^-$

Oxidation and reduction reactions occur in different areas of the metal surface, where a transfer or release of ions occurs through the electrolyte solution and the metal substrate. In the case of titanium alloys, the metal's resistance to corrosion is due to the presence of a passive oxide layer formed due to the oxidation reaction of titanium with oxygen molecules. The stability and thickness of the passive oxide layer formation depend on the metal electrochemical potential and the titanium oxidizing ability. However, this passive oxide layer is very easily damaged [33].

The passive layer on metallic biomaterials in Hanks' solution is a system consisting of both active and passive surfaces, which are simultaneously in contact with the electrolyte. Due to contact with the electrolyte solution, the passive oxide layer undergoes dissolution and re-deposition in the solution. If the dissolution rate is higher than the deposition rate, ions are released [29]. This process is called anodic dissolution. The high potential for oxidation of metallic materials at the anode can encourage an increase in the dissolution rate, which causes many ions to be released into the solution.

The dissolution rate of TiO_2 is as follows:

Oxidation: $Ti + O_2 \rightarrow TiO_2$

Reduction: $2H_2O \rightarrow O_2 + 4\,e + 4H^+$

$TiO_2 + 6Cl^- + 4H^+ \rightarrow [TiCl]_6^{2-} + 2H_2O$

$Ti^{4+} + 6Cl^- \rightarrow [TiCl]_6^{2-}$

Cl in Hanks' solution can produce Cl^- ions, which can then enter the pores of the TiO_2 layer found on the surface of TNTZ and then form complex compounds and cause the TiO_2 layer to get thinner and continue to decrease or even run out as the concentration of the complex compounds that bind Ti^{4+} ions to Cl^- increases. The results of this study indicate that thermomechanical treatment of TNTZ significantly suppresses the corrosion rate. As explained earlier, before being treated thermomechanically, TNTZ had fine pores into which ions in Hanks' solution easily penetrated, causing corrosion. The treatment, which was then applied to TNTZ, finally made the pores denser and much reduced so that the ions in Hanks' solution could not enter, thereby reducing or preventing the corrosion. This mechanism was evidenced by the research showing that TNTZ's corrosion rate and the concentration of metal ions released into Hank's solution were significantly reduced after thermomechanical treatment.

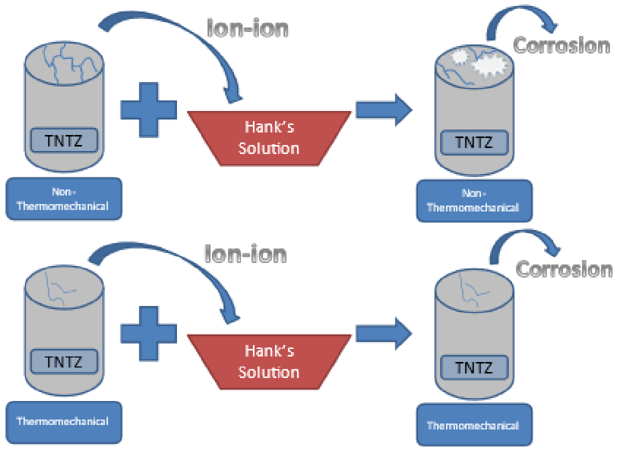

Fig. 11 Illustration of the mechanism of effect of thermomechanical treatment on TNTZ on corrosion

The mechanism of thermomechanical treatment can be illustrated in Figure 11. TNTZ without thermomechanical treatment was immersed in Hanks' solution. Because it still had pores or gaps, the ions in Hanks' solution were easy to enter and caused the corrosion process and the release of metal ions from TNTZ into the Hanks solution. Meanwhile, TNTZ with thermomechanical treatment had a tighter structure that prevented the formation of gaps or pores for ions from Hanks' solution to enter, causing the corrosion process to be reduced or hampered and causing the rate of release of metal ions from TNTZ into Hanks' solution to reduce as well.

The research results also show that the greater the deformation in the thermomechanical treatment, the higher the material density. In Figure 12, before the thermomechanical treatment, the average density of TNTZ was 6.82 g/cm^3, which increased after the thermomechanical process with deformations of 10%, 15%, and 20% to 7.65 g/cm^3, 8.09 g/cm^3, and 8.77 g/cm^3, respectively. The greater the deformation in the thermomechanical treatment, the denser the material, thereby increasing the corrosion resistance, as shown in Table 7. This finding agreed with previous studies, saying that the greater the deformation in the thermomechanical treatment, the greater the corrosion resistance [14]. Thermomechanical treatment increases the material density but does not change its crystal structure (unit cell) [21]. Phase β TNTZ titanium has a BCC (body-centered cubic) unit cell with an atomic density factor (APF) arrangement of 68% [32].

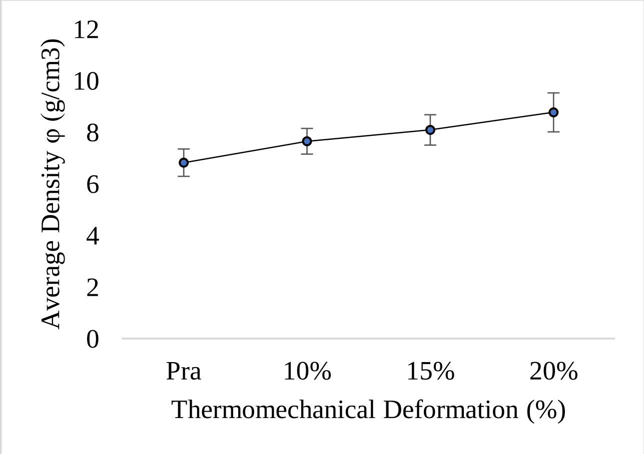

Fig. 12 Density of thermomechanical treatment TNTZ

4. Conclusion

Based on the research, it can be concluded that:

1. Thermomechanical treatment has been proven to effectively prevent the corrosion in TNTZ material based on the analysis that showed the decreasing of numbers of pit that found TNTZ samples. These findings indicate that the treatment could reduce pitting corrosion. The results of the EDX examination also showed that the elements released post-corrosion after thermomechanical treatment were less than those before the treatment.

2. The results of the corrosion rate test showed that TNTZ was still better than other materials at corrosion resistance. Also, thermomechanical treatment could reduce TNTZ' corrosion rate, which decreased along with the increase in deformation rates. The most valuable reduction in corrosion rate occurred at a deformation level of 20%. This was indicated by the lower corrosion current density (Icorr) and the greater corrosion stress (Ecorr) that means the corrosion rate was lower than before the thermomechanical treatment. Overall, the results of this study indicated that TNTZ resulting from thermomechanical treatment is the best material for use in biomedical applications compared to other materials.

4.1. Recommendations and Future Research

1. Thermomechanical treatment can improve the corrosion resistance of titanium materials; however, there is still a problem to overcome which is the pitting corrosion that is found in TNTZ that probably occurs due to the pressing process that conducted at room temperature could prevent the homogenization process from reaching its optimal state. For this reason, future research should conduct mechanical loading with hot forging below the β transus temperature to further enhance the homogenization process and reduce element separation to prevent elements from being released and producing holes (reduction in volume).

2. The amount of metal ions released due to corrosion is also important to know because the higher metal ions released will increase the toxicity that causes allergies and other biological effects, which must be considered for the safety of metal biomaterials. The release of metal ions the body in the amount exceeding 1 ppm can result in the formation of toxins (poisons) in the body. Due to the important effect of the released metal ions on the body, further research on the amount and characteristics of the released ions is important and useful to control the release triggered by, in particular, corrosion.

References

[1] WIDYASTUT. Synthesis and Characterization of Carbonated Hydroxyapatite as Bioceramic Material, Thesis, *School of Materials and Mineral Resources Engineering Universiti Sains Malaysia*, Penang, 1-2, 2009. http://scholar.unand.ac.id/36277/

[2] LARSSON T F, MARTINEZ J M M, and VALLES J L. Biomaterials for Healthcare a Decade of Eu-Funded Research. *Directorate-General for Research, Industrial technologies Unit G3* 'Value – Added Materials. EUR 22817, 2007.

[3] ASTM Handbook. *Standard Specification for Wrought 18Chromium-14Nickel-2.5Molybdenum Stainless Steel Bar and Wire for Surgical Implants* (UNS S31673). Ohio: ASTM International Vol. 3: 103-115, 2011.

[4] UMARDHANI Y, & SUPRIHANTO A. Pengembangan Metode Peningkatan Kekerasan Baja Tahan Karat Aisi 316L Lewat Proses Nitridasi Gas Temperatur Tinggi, Rotasi, 2013, 15(1): 7-10. https://ejournal.undip.ac.id/index.php/rotasi/article/view/4648

[5] HAFIZI I, WIDJIJONO W, & SOESATYO M H N E. Penentuan konsentrasi stainless steel 316L dan kobalt kromium remanium GM-800 pada uji GPMT. *Majalah Kedokteran Gigi Indonesia*, 2016, 2(3): 121. https://journal.ugm.ac.id/mkgi/article/view/11386

[6] ASTM Handbook. *Standard Specification for Wrought Titanium-6Aluminum-4Vanadium ELI (Extra Low Interstitial) Alloy for Surgical Implant Applications* (UNS R56401). Ohio: ASTM International Vol. 2: 67-89, 2011.

[7] BOSE S, PATHAK L C, & SINGH R. Response of Boride Coating on the Ti-6Al-4V Alloy to Corrosion and Fretting Corrosion Behavior in Ringer's Solution for Bio-Implant Application, *Applied Surface Science*, 2017, 433: 1158-1174. https://www.sciencedirect.com/science/article/pii/S0169433217328714

[8] ROKHMANTO, F, SENOPATI G, SUTOWO C, et al. Perlakuan Termomekanikal Ingot Paduan Co-26Cr-6Mo-0,18N. Prosiding Seminar Nasional Sains Dan Teknologi, November 2016, 1–6. https://jurnal.umj.ac.id/index.php/semnastek/article/view/2047

[9] MACFUDZOH P A, AMIN M N, & PUTRI L S D. Efektivitas Ekstrak Daun Belimbing Wuluh sebagai Bahan Inhibitor Korosi pada Kawat Ortodonsi Berbahan Dasar Nikel-Titanium. Jurnal Fakultas Kedokteran Gigi, Universitas Jember, 2014: 1-6. https://repository.unej.ac.id/handle/123456789/59393

[10] GUNAWARMAN, NIINOMI M, EYLON D, et al.

Effect of β Phase Stability at Room Temperature on Mechanical Properties in β Rich α+β Type Ti–4.5Al–3V–2Mo–2Fe Alloy. *ISIJ International*, 2002, 42(2): 191-199. https://www.jstage.jst.go.jp/article/isijinternational1989/42/2/42_2_191/_article/-char/ja/

[11] NIINOMI M. Biologically and Mechanically Biocompatible Titanium Alloys, Special Issue on Advanced Light Metals and Processing in Asia. *The Japan Institute of Light Metals, Materials Transactions*, 2008, 49(10): 2170-2178. https://www.jstage.jst.go.jp/article/matertrans/49/10/49_L-MRA2008828/_article/-char/ja/

[12] MOHAMMED M T, KHAN Z A, & SIDDIQUEE A N. Beta Titanium Alloys: The Lowest Elastic Modulus for Biomedical Applications: A Review. *World Academy of Science, Engineering and Technology International Journal of Chemical, Nuclear, Metallurgical and Materials Engineering* 2014, 8(8): 726-731.

[13] NIINOMI, M, NAKAI, M, & HIEDA, J, Development of new metallic alloys for biomedical applications. *Acta Biomaterialia*, 2012, 8: 3888-3903. https://www.sciencedirect.com/science/article/pii/S1742706112002942

[14] AKAHORI T, NIINOMI M, FUKUI H, & SUZUKI A. Fatigue, fretting fatigue and corrosion characteristics of biocompatible bet type titanium alloy conducted with various thermo-mechanical treatments. *Materials Transactions*, 2004, 45(5), 1540-1548. https://www.jstage.jst.go.jp/article/matertrans/45/5/45_5_1540/_article/-char/ja/

[15] KARTHEGA M, RAHMAN V, & RAJENDRAN N. Influence of Potential on the Electrochemical Behavior of ß Titanium Alloys in Hank's Solution, Elsevier, *Acta Biomaterialia*, 2007, 3: 1019-1023. https://www.sciencedirect.com/science/article/pii/S1742706107000323

[16] RAHMAN V, NAGARAJAN S, & RAJENDRAN N. Electrochemical Impedance Spectroscopic Characterization of Passive Film Formed Over ß Ti-29Nb-13Ta-4,6Zr Alloy, Elsevier, *Electrochemistry Communications*, 2006, 8: 1309-1314.

[17] GUNAWARMAN J A, REFIESKA A, ILHAMDI, et al. Corrosion behavior of new beta type Ti-29Nb-13Ta-4.6Zr alloy in simulated body fluid solution, *Frontiers in Bioengineering and Biotechnology*, 2016. 10th World Biomaterials Congress. doi: 10.3389/conf.FBIOE.2016.01.01060

[18] SIR ANDERSON, AMIN A S P, AFFI J, et al. Corrosion Characteristics of Titanium TNTZ And Ti-6Al-4V ELI in Artificial Saliva Solution at Human Body Temperature. *International Journal of Scientific and Technology Research*, 2021, 10(04): 240-245.

[19] REZA ASGARI BIDHENDI H, & POURANVARI M. Corrosion Study of Metallic Biomaterials in Simulated Body Fluid. *Metallurgical and Materials Engineering*, 2011, 17(1): 13-22. https://doi.org/10.30544/384

[20] SIR ANDERSON, ANNISA, AFFI J, et al. The Effect of Aging Treatment on Mechanical Properties and Microstructures of Ti-12Cr in Ortodontic Applications. *IOP Conference Series: Materials Science and Engineering*, 2020, 846: 012066. https://iopscience.iop.org/article/10.1088/1757-899X/846/1/012066/meta

[21] MOTYKA M, & SIENIAWSKI J. The influence of initial plastic deformation on microstructure and hot plasticity of α+β titanium alloys. *Archives of Materials Science and Engineering*, 2010, 41(2): 95-103. http://www.amse.acmsse.h2.pl/vol41_2/4124.pdf

[22] SIR ANDERSON, FERNANDO E, AFFI J, et al. Effect of Thermomechanical Treatment on Mechanical Properties and Microstructure of Titanium Alloy Ti-6AL-4V ELI for Orthopedic Applications. *International Journal on Advanced Science, Engineering, and Informational Technology*, 2021, 11(6): 2271-2278.

[23] SIR ANDERSON, AL-BAYUMMY T A, AFFI J, et al. Improvement of the Corrosion Resistance and Potential for Metal Ion Release of Titanium Alloy Ti-6Al-4V ELI in Hanks Balanced Salt Solution (HBSS) after Thermomechanical. *Materials Science Forum*, 2022, 1057: 176-188. https://www.scientific.net/MSF.1057.176

[24] NIINOMI M, AKAHORI T, SHIGEKI KATSURA S, et al. Mechanical characteristics and microstructure of drawn wire of Ti–29Nb–13Ta–4.6Zr for biomedical applications. *Materials Science and Engineering: C*, 2007, 27(1), 154-161. https://www.sciencedirect.com/science/article/pii/S0928493106000580

[25] NAKAI M, NIINOMI M, & ONEDA T. Improvement in Fatigue Strength of Biomedical β-type Ti–Nb–Ta–Zr Alloy While Maintaining Low Young's Modulus Through Optimizing ω-Phase Precipitation, *Metallurgical and Materials Transactions* A, 2012, 43: 294–302.

[26] BOYER R, WELSCH G, and COLLINGS E W. *Materials Properties Handbook: Titanium Alloys*. ASM International, 1994: 65–74.

[27] TAMILSELVI S, RAMAN V, & RAJENDRAN N. Corrosion Behavior of Ti-6Al-7Nb and Ti-6Al-4V ELI Alloys in the Simulated Body Solution by Electrochemical Impedance Spectroscopy, *Electrochimica Acta*, 2006, 52: 839-846. https://www.sciencedirect.com/science/article/pii/S0013468606006888

[28] TALHA M, BEHERA C K, & SINHA O P. Potentiodynamic polarization study of Type 316L and 316LVM stainless steels for surgical implants in simulated body fluids. *Journal of Chemical and Pharmaceutical Research*, 2012, 4: 203-208.

[29] HANAWA T. Metal ion release from metal implants, *Materials Science and Engineering* C, 2004, 24, 745-52, https://www.sciencedirect.com/science/article/pii/S0928493104000906

[30] RUSSEL W, and SIMON B. *Fatigue of Beta Processed and Beta Heat Treated Titanium Alloy*. 2012.

[31] DONACHIE M J. *Heat Treating Titanium and Its Alloys*. Heat Treating Progress, 2001. https://www.sciencedirect.com/science/article/pii/S0038092X18307333

[32] CALLISTER JR W D, & RETHWISCH D G. *Materials Science and Engineering: An Introduction*, 10th Edition, 2018. https://www.mse.ufl.edu/wp-content/uploads/EMA-6001-F19-Syllabus_Basim.pdf

[33] BOCCHETTA P, CHEN L-Y, TARDELLI J D C, et al. Passive Layers and Corrosion Resistance of Biomedical Ti-6Al-4V and β-Ti Alloys. *Coatings MDPI*, 2021, 11: 487. https://www.mdpi.com/2079-6412/11/5/487

参考文:

[1] WIDYASTUT. 碳酸羟基磷灰石作为生物陶瓷材料的合成与表征，论文，马来西亚理科大学材料与矿产资源工程学院，槟城，2009。http://scholar.unand.ac.id/36277/

[2] LARSSON T F、MARTINEZ J M M, 和 VALLES J L. 欧盟资助研究十年的医疗保健生物材料。工业技术研究总局 G3 部门“增值材料”。22817 欧元，2007。

[3] ASTM 手册。外科植入物用锻造 18 铬-14 镍-2.5 钼不锈钢棒材和线材的标准规范(联合国系统 S31673)。俄亥俄州：ASTM 国际卷。3: 103-115, 2011。

[4] UMARDHANI Y, 和 SUPRIHANTO A. 爱斯 316 大号不锈钢高温气体渗氮增硬度方法的开发，轮换，2013, 15(1): 7-10. https://ejournal.undip.ac.id/index.php/rotasi/article/view/4648

[5] HAFIZI I, WIDJIJONO W, 和 SOESATYO M H N E. 个人意见不锈钢 GPMT 测试中的 316 大号和通用汽车-800 钴铬再生金属。牙科杂志印度尼西亚，2016 年，2(3)：121。https://journal.ugm.ac.id/mkgi/article/view/11386

[6] ASTM 手册。用于外科植入物应用的锻造钛 6 铝 4 钒英语语言学（超低间隙）合金的标准规范（联合国系统 R56401)。俄亥俄州：ASTM 国际卷。2: 67-89, 2011.

[7] BOSE S, PATHAK L C, 和 SINGH R. Ti-6Al-4V 合金上的硼化物涂层对生物植入物林格溶液中腐蚀和微动腐蚀行为的响应，应用表面科学，2017，433：1158- 1174. https://www.sciencedirect.com/science/article/pii/S0169433217328714

[8] ROKHMANTO, F, SENOPATI G, SUTOWO C, 等。合金锭 Co-26Cr-6Mo-0.18N 的热机械处理。全国科学技术研讨会论文集，2016, 11，1-6。https://jurnal.umj.ac.id/index.php/semnastek/article/view/2047

[9] MACFUDZOH P A、AMIN M N 和 PUTRI L S D. 北林武禄叶提取物作为镍钛正畸线腐蚀抑制剂的有效性。任抹大学牙科学院学报，2014：1-6。https://repository.unej.ac.id/handle/123456789/59393

[10] GUNAWARMAN、NIINOMI M、EYLON D 等。室温下 β 相稳定性对富 β α+β 型 Ti–4.5Al–3V–2Mo–2Fe 合金力学性能的影响。ISIJ 国际, 2002, 42(2): 191-199. https://www.jstage.jst.go.jp/article/isijinternational1989/42/2/42_2_191/_article/-char/ja/

[11] NIINOMI M. 生物和机械生物相容性钛合金，亚洲先进轻金属和加工特刊。日本轻金属学会，材料交易，2008, 49(10): 2170-2178。https://www.jstage.jst.go.jp/article/matertrans/49/10/49_L-MRA2008828/_article/-char/ja/

[12] MOHAMMED M T、KHAN Z A 和 SIDDIQUEE A N. 测试版钛合金：生物医学应用的最低弹性模量：综述。世界科学院工程技术国际化学核冶金材料工程杂志 2014, 8(8): 726-731.

[13] NIINOMI, M, NAKAI, M, 和 HIEDA, J，用于生物医学应用的新型金属合金的开发。 生物材料学报, 2012, 8: 3888-3903. https://www.sciencedirect.com/science/article/pii/S1742706112002942

[14] AKAHORI T, NIINOMI M, FUKUI H, 和 SUZUKI A. 通过各种热机械处理进行的生物相容性 bet 型钛合金的疲劳、微动疲劳和腐蚀特性。材料交易，2004, 45(5), 1540-1548。https://www.jstage.jst.go.jp/article/matertrans/45/5/45_5_1540/_article/-char/ja/

[15] KARTHEGA M, RAHMAN V, 和 RAJENDRAN N. 电位对汉克溶液中 ß 钛合金电化学行为的影响，生物材料学报，2007，3：1019-1023。https://www.sciencedirect.com/science/article/pii/S1742706107000323

[16] RAHMAN V、NAGARAJAN S 和 RAJENDRAN N. 在 ß Ti-29Nb-13Ta-4,6Zr 合金上形成的钝化膜的电化学阻抗光谱表征，爱思唯尔，电化学通讯，2006，8：1309-1314。

[17] GUNAWARMAN J A、REFIESKA A、ILHAMDI 等。新型 β 型 Ti-29Nb-13Ta-4.6Zr 合金在模拟体液溶液中的腐蚀行为，生物工程与生物技术前沿，2016。第十届世界生物材料大会。土井：10.3389/conf.FBIOE.2016.01.01060

[18] SIR ANDERSON, AMIN A S P, AFFI J, 等。钛天梯和 Ti-6Al-4V 英语语言学在人体温度下人工唾液溶液中的腐蚀特性。国际科学技术研究杂志, 2021, 10(04): 240-245.

[19] REZA ASGARI BIDHENDI H, 和 POURANVARI M. 金属生物材料在模拟体液中的腐蚀研究。冶金与材料工程, 2011, 17(1): 13-22. https://doi.org/10.30544/384

[20] SIR ANDERSON, ANNISA, AFFI J, 等。正畸应用中时效处理对 Ti-12Cr 机械性能和微观结构的影响。眼压会议系列：材料科学与工程，2020，846：012066。https://iopscience.iop.org/article/10.1088/1757-899X/846/1/012066/meta

[21] MOTYKA M, 和 SIENIAWSKI J. 初始塑性变形对 α+β 钛合金微观结构和热塑性的影响。材料科学与工程档案，2010, 41(2): 95-103. http://www.amse.acmsse.h2.pl/vol41_2/4124.pdf

[22] SIR ANDERSON, FERNANDO E, AFFI J, 等。热机械处理对用于骨科应用的钛合金 Ti-6AL-4V 英语语言学

的机械性能和微观结构的影响。国际先进科学、工程和信息技术杂志, 2021, 11(6): 2271-2278.

[23] SIR ANDERSON, AL-BAYUMMY T A, AFFI J, 等。热机械后钛合金 Ti-6Al-4V 英语语言学在汉克斯平衡盐溶液(哈佛商学院)中的耐腐蚀性和金属离子释放潜力的提高。材料科学论坛, 2022, 1057: 176-188. https://www.scientific.net/MSF.1057.176

[24] NIINOMI M, AKAHORI T, SHIGEKI KATSURA S, 等。用于生物医学应用的 Ti-29Nb-13Ta-4.6Zr 拉丝的机械特性和微观结构。材料科学与工程: C, 2007, 27(1), 154-161. https://www.sciencedirect.com/science/article/pii/S0928493106000580

[25] NAKAI M, NIINOMI M, 和 ONEDA T. 在优化 ω 相析出的同时保持低杨氏模量的生物医用 β 型钛铌钽锆合金的疲劳强度提高，冶金和材料交易一种，2012，43：294-302。

[26] BOYER R、WELSCH G 和 COLLINGS EW. 材料特性手册：钛合金。ASM 国际，1994：65-74。

[27] TAMILSELVI S、RAMAN V 和 RAJENDRAN N. Ti-6Al-7Nb 和 Ti-6Al-4V 英语语言学合金在模拟人体溶液中的电化学阻抗谱腐蚀行为，电化学学报，2006，52：839-846 。https://www.sciencedirect.com/science/article/pii/S0013468606006888

[28] TALHA M、BEHERA C K 和 SINHA OP P. 模拟体液中外科植入物用 316 大号和 316LVM 不锈钢的动电位极化研究。化学与药物研究杂志，2012，4：203-208。

[29] HANAWA T. 金属植入物的金属离子释放，材料科学与工程 C，2004，24 日，745-52，https://www.sciencedirect.com/science/article/pii/S0928493104000906

[30] RUSSEL W 和 SIMON B. 测试版处理和测试版热处理钛合金的疲劳。 2012.

[31] DONACHIE M J. 热处理钛及其合金。热处理进展，2001 。https://www.sciencedirect.com/science/article/pii/S0038092X18307333

[32] CALLISTER JR W D 和 RETHWISCH D G. 材料科学与工程：简介，第 10 版，2018 。https://www.mse.ufl.edu/wp-content/uploads/EMA-6001-F19-Syllabus_Basim.pdf

[33] BOCCHETTA P、CHEN L-Y、TARDELLI J DC 等。生物医用 Ti-6Al-4V 和β-钛合金的钝化层和耐蚀性。涂料 MDPI，2021，11:487。https://www.mdpi.com/2079-6412/11/5/487